

Adaptive Prescribed-Time Neural Control of Nonlinear Systems via Dynamic Surface Technique

Wang, Ping; Yu, Chengpu; Lv, Maolong; Zhao, Zilong

DOI

[10.1109/TAI.2024.3404914](https://doi.org/10.1109/TAI.2024.3404914)

Publication date

2024

Document Version

Final published version

Published in

IEEE Transactions on Artificial Intelligence

Citation (APA)

Wang, P., Yu, C., Lv, M., & Zhao, Z. (2024). Adaptive Prescribed-Time Neural Control of Nonlinear Systems via Dynamic Surface Technique. *IEEE Transactions on Artificial Intelligence*, 5(10).
<https://doi.org/10.1109/TAI.2024.3404914>

Important note

To cite this publication, please use the final published version (if applicable).
Please check the document version above.

Copyright

Other than for strictly personal use, it is not permitted to download, forward or distribute the text or part of it, without the consent of the author(s) and/or copyright holder(s), unless the work is under an open content license such as Creative Commons.

Takedown policy

Please contact us and provide details if you believe this document breaches copyrights.
We will remove access to the work immediately and investigate your claim.

Green Open Access added to TU Delft Institutional Repository

'You share, we take care!' - Taverne project

<https://www.openaccess.nl/en/you-share-we-take-care>

Otherwise as indicated in the copyright section: the publisher is the copyright holder of this work and the author uses the Dutch legislation to make this work public.

Adaptive Prescribed-Time Neural Control of Nonlinear Systems via Dynamic Surface Technique

Ping Wang , Chengpu Yu , Senior Member, IEEE, Maolong Lv , and Zilong Zhao 

Abstract—The adaptive practical prescribed-time (PPT) neural control is studied for multiinput multioutput (MIMO) nonlinear systems with unknown nonlinear functions and unknown input gain matrices. Unlike existing PPT design schemes based on backstepping, this study proposes a novel PPT control framework using the dynamic surface control (DSC) approach. First, a novel nonlinear filter (NLF) with an adaptive parameter estimator and a piecewise function is constructed to effectively compensate for filter errors and facilitate prescribed-time convergence. Based on this, a unified DSC-based adaptive PPT control algorithm, augmented with a neural networks (NNs) approximator, is developed, where NNs are used to approximate unknown nonlinear system functions. This algorithm not only addresses the inherent computational complexity explosion associated with traditional backstepping methods but also reduces the constraints on filter design parameters compared to the DSC algorithm that relies on linear filters. The simulation showcases the effectiveness and superiority of the devised scheme by employing a two-degree-of-freedom robot manipulator.

Impact Statement—Due to the increased demand for intelligence and autonomy development, intelligent control of nonlinear systems has gained widespread attention and has been extensively explored and applied across various practical fields. In particular, the prescribed-time (PT) intelligent control, which aims to restore the system state to a stable state within a specified time, holds significant practical research value as it guarantees the rapid convergence of the system. However, there are few PT intelligent control results for MIMO nonlinear systems with unknown nonlinear functions and unknown input gain matrices. Henceforth, based on the dynamic surface technology, this study

proposes a PT neural control scheme by constructing a new NLF, which effectively achieves the prescribed-time convergence of tracking errors. This framework not only avoids the inherent computational complexity explosion associated with traditional backstepping but also reduces the constraints on filter design parameters. Finally, the algorithm's practicality and superiority are validated through simulation examples, demonstrating its potential for further extension to real-world applications.

Index Terms—Dynamic surface control (DSC), nonlinear filter (NLF), nonlinear system, prescribed-time (PT) neural control, robot manipulator.

I. INTRODUCTION

PRESCRIBED-TIME (PT) control, proposed in [1] and [2], has gained significant attention in recent years [3], [4], [5], [6], [7], injecting new life into the control field. PT control is appealing due to the fact that, unlike existing finite-time [8], [9], [10] or fixed-time [11], [12], [13], [14], [15] control, the designer can predetermine the settling time, independent of the system initial value and control parameters. To achieve PT convergence, various effective methods have been developed in [16], [17], [18], [19], [20], [21], and [22], including the state scaling-based approach in [2], [3], [4], [16], and [17], as well as the time scaling-based scheme in [18], [19], and [20]. More recently, in [21], a linear time-varying feedback was proposed to achieve PT stabilization for nonlinear systems, using the solution of Lyapunov equations that included a function that goes to infinity as the time approaches the settling time. Additionally, in [22], a novel nonscaling backstepping design was developed for stochastic systems. However, it is noteworthy that most of these results only consider robust controls, making it challenging to handle more system uncertainties.

Adaptive control offers a promising approach for addressing uncertainty. However, ensuring the boundedness of parameter estimation, as highlighted in [23], poses challenges in designing controllers with PT stability. To tackle this issue, researchers have recently proposed several innovative adaptive PT control methods. For instance, in [24], dynamic high-gain state scaling approach was employed to achieve adaptive PT stabilization for uncertain nonlinear systems. In [25], a newly PT control framework was presented, eliminating the reliance on time-varying functions for state transformations and thereby reducing computational burdens compared to the approach in [24]. Another study, [26], designed a DSC-based adaptive PT control utilizing

Manuscript received 13 December 2023; revised 18 February 2024 and 27 March 2024; accepted 18 May 2024. Date of publication 24 May 2024; date of current version 15 October 2024. This work was supported in part by the National Key Research and Development Project under Grant 2020YFC1512503, in part by the National Natural Science Foundation of China under Grant 61991414, in part by Chongqing Natural Science Foundation under Grant CSTB2023NSCQ-JQX0018, in part by Beijing Natural Science Foundation under Grant L221005, in part by the Natural Science Basic Research Program of Shaanxi under Program 2024JC-YBQN-0668, in part by the Project for Science and Technology under Grant 2022-JCJQ-QT-018, in part by Young Talent Fund of Association for Science and Technology in Shaanxi under Grant 20220101, and in part by the Postdoctoral International Exchange Project under Grant YJ20220347. (Corresponding author: Chengpu Yu.)

Ping Wang and Chengpu Yu are with the School of Automation, Beijing Institute of Technology, Beijing 100081, China, and also with Beijing Institute of Technology Chongqing Innovation Center, Chongqing 401120, China (e-mail: pingwang0906@126.com; yuchengpu@bit.edu.cn).

Maolong Lv is with the College of Air Traffic Control and Navigation, Air Force Engineering University, Xi'an 710051, China (e-mail: maolonglv@163.com).

Zilong Zhao is with the Faculty of Electrical Engineering Mathematics and Computer Science, Delft University of Technology, 2628 CD Delft, The Netherlands (e-mail: z.zhao-8@tudelft.nl).

Digital Object Identifier 10.1109/TAI.2024.3404914

TABLE I
COMPARISON BETWEEN THIS STUDY AND SOME REPRESENTATIVE ADAPTIVE PT CONTROL RESULTS

Ref.	System model			System uncertainty			Control method		
	SISO	MIMO		Parameter uncertainty	Unknown control gain	Unknown nonlinear	Backstepping	DSC	
		Second-order	High-order					Linear filter	Nonlinear filter
[24], [31]	✓					✓	✓		
[25]	✓			✓			✓		
[26]	✓			✓				✓	
[27]		✓		✓	✓		✓		
[28], [29]	✓				✓		✓		
[33]		✓			✓	✓	✓		
[34]		✓			✓	✓		✓	
[35]			✓	✓	✓		✓		
[36]			✓	✓	✓		✓		
Our article			✓	✓	✓	✓			✓

linear filter (LF) and state scaling transformation for nonlinear systems. Notably, the adaptive schemes [24], [25], [26] only work for parameter uncertainties to obtain PT stabilization performance, thus exhibiting limitations when handling other forms of uncertainties. Furthermore, although the controller designs proposed in [24], [25], and [26] are capable of driving the system state converging to origin within the prescribed time, they may result in excessive control inputs and costs in practical applications. This can be problematic for certain systems such as space rendezvous and docking teleoperation [27] where the end-effector of the space robot must reach a predefined capture area within a specific time.

To achieve PT convergence with a preset residual set for control design, the concept of practical prescribed-time (PPT) control has been proposed in single-input single-output (SISO) systems [28], [29], [30], [31], [32] and MIMO systems [33], [34], [35], [36]. In [28], the PPT tracking control was studied for normal-form nonaffine systems with nonparametric uncertainties, while a transformation-based adaptive control scheme was developed in [29] for strict-feedback systems with unknown control directions. The output-feedback PPT has also been discussed in [30] for strict-feedbacklike form with exogenous disturbance. The recent results [31], [32] achieved the event-triggered PPT control of nonlinear systems. In [33], a neural adaptive PPT tracking control scheme for Euler–Lagrange systems with full-state constraints was addressed by using the backstepping scheme. Subsequently, Cao et al. [34] presented a LF-based DSC framework for handling the PPT control for Euler–Lagrange systems with system uncertainties. While the control schemes in [31], [33], and [34] effectively handle unknown nonlinear functions, it is important to note that the PT convergence set of Lyapunov functions is dependent on control parameters, making implementation challenging in practical applications. Addressing this concern, recent research [35], [36] presented a new sufficient condition for adaptive PPT stability in nonlinear MIMO systems by constructing a new piecewise exponential function. The merit of this algorithm lies in that the convergence domain and convergence time can be decoupled

into separately user-defined parameters, which are independent of the control parameters and initial values. However, the algorithms proposed in [35] and [36] are based on the traditional adaptive backstepping process, which can lead to the explosive growth problem due to the virtual controller (VC)'s derivative in the iterative design of each step. An effective strategy for addressing the complexity explosion phenomenon is the utilization of DSC technology [37], [38], [39], which applies a first-order filter to the VC during each backstepping iteration, thus transforming the differential operation into algebraic operation. Based on our current knowledge, there is no previous research available on achieving adaptive PPT stability using DSC schemes for nonlinear MIMO systems that support user-defined convergence time and convergence region characteristics. This article aims to investigate this area and proposes new methods for achieving this goal.

Building upon the preceding discussions, this article delves into the realm of adaptive PPT stability of nonlinear MIMO systems with unknown nonlinear functions and unknown input gain matrices, employing the DSC approach. For visual clarity, Table I illustrates a comparison between the outcomes of this study and some representative adaptive PT control schemes. The primary contributions of this research are as follows.

- 1) A novel adaptive PPT scheme for uncertain MIMO nonlinear systems using the DSC framework is presented. Compared with recent PPT stability schemes [27], [33], [35], [36] that use the conventional backstepping method, our proposed control scheme avoids the computational complexity explosion by eliminating the need to calculate the VC's derivative in each iteration under the backstepping settings.
- 2) Unlike traditional DSC-based PT algorithms [26], [34] with LFs, we construct a novel nonlinear filter (NLF) incorporating a parameter estimator and a piecewise function. This filter not only effectively compensates for the filter error but also relaxes the requirement on filter parameters while ensuring PPT stability (see Remark 6).

3) Our proposed control framework integrates neural network (NN) approximation technology and adaptive control theory, making it suitable for high-order MIMO systems with more uncertainties than existing algorithms [16], [17], [18], [19], [20], [21], [22], [24], [25], [26], [27], [28], [29], [30], [31], [32], [33], [34], [35], [36]. This approach can also be expanded to address the PPT issue of MIMO systems with input saturation (See Corollary 1). Moreover, our control algorithm allows designers to preset the settling time and convergence domain separately, which is a unique feature not found in [31], [33], and [34], where the convergence domain depends on control parameters.

The article is structured as follows. Section II provides the problem statement. Section III presents the NLF construction, controller design, and stability analysis. Simulations in Section IV verify the validity of the proposed PPT control scheme, while Section V gives the conclusions.

II. PROBLEM FORMULATION AND PRELIMINARIES

This article focuses on an uncertain nonlinear high-order MIMO systems, which is described as follows:

$$\begin{cases} \dot{x}_p(t) = x_{p+1}(t) + f_p(\bar{x}_p(t)), & p = 1, \dots, n-1 \\ \dot{x}_n(t) = G(\bar{x}_n, t)u(t) + f_n(\bar{x}_n(t)) \end{cases} \quad (1)$$

where for $p = 1, \dots, n$, $x_p \in R^m$ and $u \in R^m$ denote the system state and input, respectively, $f_p(\bar{x}_p)$ are the unknown continuous functions with $\bar{x}_p = [x_1^T, x_2^T, \dots, x_p^T]^T$, $G(\cdot)$ is the unknown input gain. Set $y(t) = x_1(t)$ as the system output.

Problem: Let the trajectory of the desired system output be $x_{1d}(t)$. The control objective is to develop an adaptive tracking control scheme based on the DSC strategy for model (1), achieving the PPT stability while ensuring that the tracking error converges to a user-defined residual set within the prescribed time.

The following assumptions and preparations are required.

Assumption 1: The tracking signal x_{1d} is continuous and differentiable. In addition, the inequality $\|\dot{x}_{1d}\| \leq x_{1d}^*$ holds with $x_{1d}^* > 0$ being a constant.

Assumption 2: The input gain function $G(\cdot)$ is positive definite and bounded by $\underline{a} \leq \|G(\cdot)\| \leq \bar{a}$, where \underline{a} and \bar{a} are two unknown positive constants.

Notations: Denote $x(t)$ by x or $x(\cdot)$ for simplicity.

Lemma 1 [9]: For any positive constants o_1, o_2, o_3 , arbitrary real numbers ξ_1, ξ_2 , and a continuous function $\gamma(\cdot) > 0$, it holds $\gamma(\cdot)\xi_1^{o_1}\xi_2^{o_2} \leq o_3|\xi_1|^{(o_1+o_2)} + (o_2/o_1 + o_2)((o_1+o_2/o_1)o_3)^{-(o_1/o_2)}\gamma(\cdot)^{(o_1+o_2/o_2)}|\xi_2|^{(o_1+o_2)}$.

Lemma 2 [39]: For $\forall x \in R$ and any constant $\tau > 0$, it has $0 \leq |x| - (x^2/\sqrt{x^2 + \tau^2}) < \tau$.

NNs have excellent approximation capabilities for continuous functions [34], [40]. Specifically, any function $f(\beta)$ that satisfies continuity can be written as

$$f(\beta) = W^{*T}\phi(\beta) + \varepsilon(\beta) \quad (2)$$

where $\beta \in \mathcal{U} \subseteq R^n$, \mathcal{U} is a compact set, the ideal weight is $W^* \in R^{\iota \times m}$ with $\iota > 1$ being the neuron number, the approximation error $\varepsilon(\beta) \in R^m$ satisfies $\|\varepsilon(\beta)\| \leq \epsilon$, ϵ is a constant.

$\phi(\beta) = [\phi_1(\beta), \phi_2(\beta), \dots, \phi_\iota(\beta)]^T \in R^\iota$ with $\phi_j(\beta)$ being defined as a radial basis function (RBF)

$$\phi_j(\beta) = \exp\left[\frac{-(\beta - \nu_j)^T(\beta - \nu_j)}{v^2}\right], \quad j = 1, 2, \dots, \iota \quad (3)$$

where v is the width and $\nu_j = [\nu_{j1}, \dots, \nu_{jn}]^T$ is the center.

On the basis of NNs, the unknown nonlinear function $f_p(\bar{x}_p)$ in (1) for $p = 1, 2, \dots, n$ will be rewritten as

$$f_p(\bar{x}_p) = W_{f_p}^{*T}\phi_{f_p}(\bar{x}_p) + \varepsilon_{f_p}(\bar{x}_p) \quad (4)$$

with $W_{f_p} \in R^{r_p \times m}$, $\phi_{f_p}(\cdot) \in R^{r_p}$, and the upper bound constant of the norm $\|\varepsilon_{f_p}(\bar{x}_p)\|$ being ϵ_p .

Next, to fulfill the PPT stability of system (1), the following time-varying piecewise function [36] is introduced

$$\varsigma(t) = \begin{cases} \exp[\mu(T_e - t)] - 1, & t \in [0, T_e) \\ \exp[\mu(t - T_e)], & t \in [T_e, +\infty) \end{cases} \quad (5)$$

where T_e denotes the convergence time defined by the designer and μ represents a tuning parameter satisfying $\mu \in (0, \ln(2)/T_e]$.

Based on this function (5), the following lemma will be provided for the PPT stability.

Lemma 3 [36]: For the nonlinear system $\dot{\chi} = F(t, \chi(t))$ with $\chi(0) = \chi_0$, where the nonlinear term $F(\cdot)$ is continuously differentiable and the equilibrium point is the origin, if there is a continuous-differentiable positive-definite function $V(\chi, t)$ and scalars $d, b, c > 0$ satisfying $d > \mu, b > c$ and

$$\dot{V} \leq -\eta(t)V + \frac{b}{c} + c$$

where $\eta(t) = d + (|\dot{\varsigma}|/\varsigma)$ and d and b are the user-defined constants, then the equilibrium of system $\dot{\chi} = F(t, \chi(t))$ is PPT stable and the convergence set is $\Omega = \{\chi | V(\chi) \leq (b/\mu)\}$ for $\forall t \geq T_e$.

Remark 1: Note that the definition of $\eta(t)$ is related to the derivative of the piecewise function $\varsigma(t)$. For implementation, we define the derivative of the piecewise function $\varsigma(t)$ at the piecewise point $t = T_e$ as its right derivative at that time. Moreover, since when $t \rightarrow T_e^-$, the limit $\lim_{T_e^-} \varsigma(t) \rightarrow 0$ holds. This together the definition of $\eta(t)$ implies that $\eta(t) \rightarrow \infty$ holds. For this reason, to avoid the singularity of the term $(|\dot{\varsigma}(t)|/\varsigma(t))$ in $\eta(t)$, the following two measures used in [23] will be adopted in the implementation process: 1) replace T_e with T_e (scheduled time) $+\epsilon$ (small constant) so that the controller works at time T_e ; and 2) set an upper bound for $\eta(t)$ before the time approaching the preset time T_e .

Remark 2: Compared with the existing studies [16], [17], [18], [19], [20], [21], [22], [23], [24], [25], [26], [27], [28], [29], [30], [31], [32], [33], [34], [35], [36] that emphasize the PT control, focusing on the PT stability of model (1) has more general theoretical and application value. On the one hand, dynamics (1) can be used to describe many practical systems compared to SISO systems [18], [19], [20], [21], [22], [23], [24], [25], [26], [28], [29], [30], [31], [32], such as marine surface vessels [9], teleportation systems [27], and robot manipulators [34]. In addition, system (1) has more uncertainties than the existing results [16], [17], [18], [19], [20], [21], [22], [24],

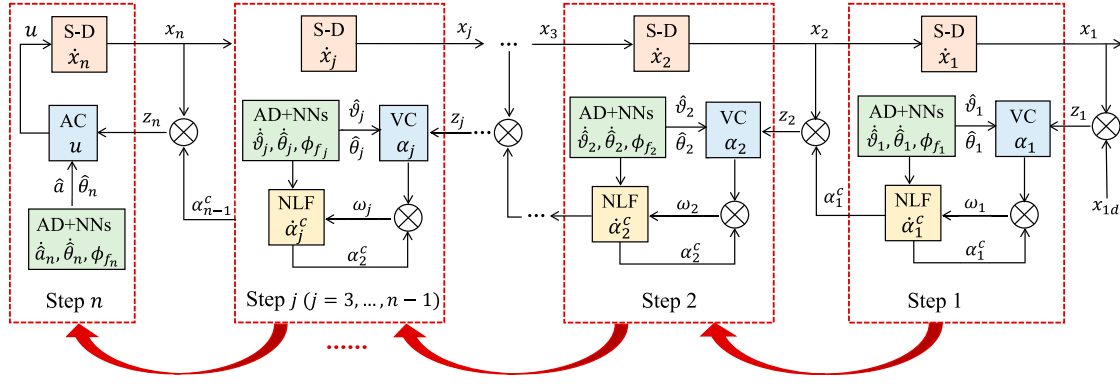


Fig. 1. Controller's iterative design flowchart.

[25], [26], [27], [28], [29], [30], [31], [32], [33], [34], [35], [36], which allows for the presence of completely unknown nonlinear functions as well as time-varying unknown input gain matrices.

III. CONTROLLER DESIGN AND STABILITY ANALYSIS

This section consists of three parts. In part A, a novel NLF designed in this article will be presented first. Based on this, the control design process and stability analysis under the settings of DSC will be subsequently discussed in part B. Finally, the main result is provided in part C.

A. NLF Design

Before the DSC design procedure, the following coordinate transformations are introduced:

$$\begin{cases} z_1 = x_1 - x_{1d} \\ z_p = x_p - \alpha_{p-1}^c \\ \omega_{p-1} = \alpha_{p-1}^c - \alpha_{p-1}, \quad p = 2, 3, \dots, n \end{cases} \quad (6)$$

where z_p is the virtual error, α_p^c is the output of the p th filter to be designed, α_p is the p th VC to be designed, and ω_p is the p th filter error. Assuming that the derivative $\dot{\alpha}_p$ is bounded by $\|\dot{\alpha}_p\| \leq \vartheta_p$ with ϑ_p being an unknown constant. Let $\hat{\vartheta}_p(t)$ be the estimate of ϑ_p and $\tilde{\vartheta}_p(t) = \vartheta_p - \hat{\vartheta}_p(t)$ be the estimation error.

Now, a novel NLF will be proposed for subsequent design procedure, which is designed as

$$\begin{cases} \rho_p \dot{\alpha}_p^c = -(\eta(t) + \frac{\rho_p}{2})\omega_p - \rho_p \hat{\vartheta}_p \frac{\omega_p}{\sqrt{\omega_p^T \omega_p + \tau_p^2}} \\ \alpha_p^c(0) = \alpha_p(0), \quad p = 1, 2, \dots, n-1 \end{cases} \quad (7)$$

where $\rho_p \in (0, 2]$, $\tau_i > 0$ are the filter time constant to be designed, and $\eta(t)$ is defined in Lemma 3. Additionally, the update equation of $\hat{\vartheta}_p$ is designed as follows:

$$\dot{\hat{\vartheta}}_p = \sigma_{\vartheta_p} \frac{\omega_p^T \omega_p}{\sqrt{\omega_p^T \omega_p + \tau_p^2}} - \eta \hat{\vartheta}_p, \quad p = 1, 2, \dots, n-1 \quad (8)$$

with $\sigma_{\vartheta_p} > 0$ being the design constant.

Remark 3: A novel NLF is designed in (7) for the subsequent controller design based on DSC, which is different from the traditional LF used in [31], [34], and [39]. Particularly, an

adaptive parameter estimator $\hat{\vartheta}_i$ updated according to (8) is included in (7), enabling the proposed DSC scheme to effectively compensate for filter errors. Additionally, the introduction of time-varying function $\eta(t)$ guarantees the convergence at the prescribed time. The advantages of the presented NLF in (7) will be further elaborated in the subsequent controller design (refer to Remark 6).

B. Controller Design Based on DSC

This section will give the controller design procedure based on DSC with the coordinate transformations in (6), the NLF in (7), and the adaptive laws in (8). The design consists of n steps, starting from the subdynamics (S-D) \dot{x}_1 , which is far away from the control input, and iteratively designing toward the S-D \dot{x}_n . Each step designs a VC α_i , ultimately achieving the design of the actual controller (AC) u . The overall iterative design flowchart is shown in Fig. 1, where ‘‘AD’’ represents an abbreviation of ‘‘adaptive.’’

Step 1: Using (1) and (6), the time derivative of z_1 is as follows:

$$\dot{z}_1 = z_2 + \omega_1 + \alpha_1 + f_1(x_1) - \dot{x}_{1d}. \quad (9)$$

On the basis of (4), let $\theta_1 = \max\{\|W_{f_1}^*\|, \epsilon_1\}$ and $\hat{\theta}_1$ be its estimate. Define the estimation error as $\tilde{\theta}_1 = \theta_1 - \hat{\theta}_1$. Then, select the first candidate Lyapunov function as

$$V_1 = \frac{1}{2} z_1^T z_1 + \frac{1}{2\sigma_{\theta_1}} \tilde{\theta}_1^2 + \frac{1}{2} \omega_1^T \omega_1 + \frac{1}{2\sigma_{\vartheta_1}} \tilde{\vartheta}_1^2 \quad (10)$$

with σ_{θ_1} and σ_{ϑ_1} being two positive design parameters. Afterwards, combining (6) and (9), the time derivative of V_1 is as follows:

$$\begin{aligned} \dot{V}_1 = & z_1^T (z_2 + \omega_1 + \alpha_1 + f_1 - \dot{x}_{1d}) - \frac{1}{\sigma_{\theta_1}} \tilde{\theta}_1 \dot{\hat{\theta}}_1 \\ & + \omega_1^T (\dot{\alpha}_1^c - \dot{\alpha}_1) - \frac{1}{\sigma_{\vartheta_1}} \tilde{\vartheta}_1 \dot{\hat{\vartheta}}_1. \end{aligned} \quad (11)$$

Set a new function $\varphi_1(x_1) = 1 + \|\phi_{f_1}(x_1)\|$ with $\phi_{f_1}(x_1)$ being defined in (4). In view of the definition of θ_1 , using Lemma 2, we can get that

$$z_1^T f_1 \leq \|z_1\| \theta_1 \varphi_1 \leq \theta_1 \tau_1 + \theta_1 \frac{z_1^T z_1 \varphi_1^2}{\sqrt{z_1^T z_1 \varphi_1^2 + \tau_1^2}}. \quad (12)$$

Based on the designed filter in (7), the definition $\tilde{\vartheta}_1 = \vartheta_1 - \hat{\vartheta}_1$ and $\|\dot{\alpha}_1\| \leq \vartheta$, combining Lemma 2 yields the following:

$$\begin{aligned} & \omega_1^T (\dot{\alpha}_1^c - \dot{\alpha}_1) \\ & \leq -\left(\frac{\eta}{\rho_1} + \frac{1}{2}\right) \omega_1^T \omega_1 - \frac{\tilde{\vartheta}_1 \omega_1^T \omega_1}{\sqrt{\omega_1^T \omega_1 + \tau_1^2}} + \|\omega_1\| \vartheta_1 \\ & \leq -\left(\frac{\eta}{\rho_1} + \frac{1}{2}\right) \omega_1^T \omega_1 + \frac{\tilde{\vartheta}_1 \omega_1^T \omega_1}{\sqrt{\omega_1^T \omega_1 + \tau_1^2}} + \vartheta_1 \tau_1. \end{aligned} \quad (13)$$

By using Lemma 1, it can be obtained that

$$z_1^T (z_2 + \omega_1) \leq z_1^T z_1 + \frac{1}{2} z_2^T z_2 + \frac{1}{2} \omega_1^T \omega_1. \quad (14)$$

Then, substituting (8) and inequalities (12)–(14) into (11), \dot{V}_1 can be further written as

$$\begin{aligned} \dot{V}_1 & \leq z_1^T \left(z_1 + \alpha_1 - \dot{x}_{1d} + \theta_1 \frac{\varphi_1^2 z_1}{\sqrt{z_1^T z_1 \varphi_1^2 + \tau_1^2}} \right) - \frac{1}{\sigma_{\theta_1}} \tilde{\theta}_1 \dot{\theta}_1 \\ & - \left(\frac{\eta}{\rho_1} + \frac{1}{2}\right) \omega_1^T \omega_1 + \frac{\tilde{\vartheta}_1 \omega_1^T \omega_1}{\sqrt{\omega_1^T \omega_1 + \tau_1^2}} + \vartheta_1 \tau_1 + \theta_1 \tau_1 \\ & - \frac{1}{\sigma_{\vartheta_1}} \tilde{\vartheta}_1 \left(\frac{\sigma_{\vartheta_1} \omega_1^T \omega_1}{\sqrt{\omega_1^T \omega_1 + \tau_1^2}} - \eta \hat{\vartheta}_1 \right) + \frac{1}{2} z_2^T z_2 + \frac{1}{2} \omega_1^T \omega_1. \end{aligned} \quad (15)$$

Design the VC α_1 as

$$\begin{aligned} \alpha_1 & = -z_1 - \frac{\hat{\theta}_1 \varphi_1^2 z_1}{\sqrt{z_1^T z_1 \varphi_1^2 + \tau_1^2}} + \dot{x}_{1d} \\ & - \frac{1}{2} \eta z_1 + \left(\frac{b}{\varsigma} - \eta^2\right) \frac{z_1}{z_1^T z_1} \end{aligned} \quad (16)$$

with b being the user-defined parameters. Select the update equation of the adaptive estimator $\hat{\theta}_1$ as

$$\dot{\hat{\theta}}_1 = \sigma_{\theta_1} \frac{\varphi_1^2 z_1^T z_1}{\sqrt{z_1^T z_1 \varphi_1^2 + \tau_1^2}} - \eta \hat{\theta}_1. \quad (17)$$

Moreover, according to Lemma 1, combined with the definitions of $\tilde{\vartheta}_1$ and $\tilde{\theta}_1$, the following inequalities can be derived

$$\begin{aligned} \frac{\eta}{\sigma_{\vartheta_1}} \tilde{\vartheta}_1 \dot{\vartheta}_1 & = -\frac{\eta}{\sigma_{\vartheta_1}} \tilde{\vartheta}_1^2 + \frac{\eta}{\sigma_{\vartheta_1}} \tilde{\vartheta}_1 \vartheta_1 \\ & \leq -\frac{\eta}{2\sigma_{\vartheta_1}} \tilde{\vartheta}_1^2 + \frac{\eta^2}{2} + \frac{\vartheta_1^4}{8\sigma_{\vartheta_1}^2} \end{aligned} \quad (18)$$

$$\frac{\eta}{\sigma_{\theta_1}} \tilde{\theta}_1 \dot{\theta}_1 \leq -\frac{\eta}{2\sigma_{\theta_1}} \tilde{\theta}_1^2 + \frac{\eta^2}{2} + \frac{\theta_1^4}{8\sigma_{\theta_1}^2}. \quad (19)$$

As a result, from (16) and (17) and inequalities (18) and (19), we can further obtain that

$$\begin{aligned} \dot{V}_1 & \leq -\frac{1}{2} \eta z_1^T z_1 + \frac{b}{\varsigma} - \frac{1}{2\sigma_{\theta_1}} \eta \tilde{\theta}_1^2 - \frac{1}{2\sigma_{\vartheta_1}} \eta \tilde{\vartheta}_1^2 \\ & - \frac{1}{\rho_1} \eta \omega_1^T \omega_1 + \frac{1}{2} z_2^T z_2 + c_1 \end{aligned} \quad (20)$$

where $c_1 = \vartheta_1 \tau_1 + \tau_1 \theta_1 + (\theta_1^4/8\sigma_{\theta_1}^2) + (\vartheta_1^4/8\sigma_{\vartheta_1}^2)$ is a positive constant.

Step j ($j = 2, 3, \dots, n-1$): By using (1) and coordinate transformations in (6), the dynamic \dot{z}_j satisfies the following:

$$\dot{z}_j = z_{j+1} + \omega_j + \alpha_j + f_j(\bar{x}_j) - \dot{\alpha}_{j-1}^c. \quad (21)$$

Similar to the first step, by using the NNs approximation (4), let $\theta_j = \max\{\|W_{f_j}^*\|, \epsilon_j\}$ and define the estimation error as $\theta_j = \theta_j - \hat{\theta}_j$, where $\hat{\theta}_j$ is the estimate of θ_j . Then, construct the j th Lyapunov function as

$$V_j = V_{j-1} + \frac{1}{2} z_j^T z_j + \frac{1}{2\sigma_{\theta_j}} \tilde{\theta}_j^2 + \frac{1}{2} \omega_j^T \omega_j + \frac{1}{2\sigma_{\vartheta_j}} \tilde{\vartheta}_j^2 \quad (22)$$

where σ_{θ_j} and σ_{ϑ_j} are two positive parameters to be designed. Besides, we can obtain the following inequality from step $j-1$ by inductive method:

$$\begin{aligned} \dot{V}_{j-1} & \leq \sum_{m=1}^{j-1} \eta \left(-\frac{1}{2} z_m^T z_m - \frac{1}{2\sigma_{\theta_m}} \tilde{\theta}_m^2 - \frac{1}{2\sigma_{\vartheta_m}} \tilde{\vartheta}_m^2 \right. \\ & \left. - \frac{1}{\rho_m} \omega_m^T \omega_m \right) + \frac{b}{\varsigma} + \frac{1}{2} z_j^T z_j + c_{j-1} \end{aligned} \quad (23)$$

with $c_{j-1} = \sum_{m=1}^{j-1} (\vartheta_m \tau_m + \tau_m \theta_m + (\theta_m^4/8\sigma_{\theta_m}^2) + (\vartheta_m^4/8\sigma_{\vartheta_m}^2))$.

Next, using (7) and (21) yield the following:

$$\begin{aligned} \dot{V}_j & = \dot{V}_{j-1} + z_j^T (z_{j+1} + \omega_j + \alpha_j + f_j - \dot{\alpha}_{j-1}^c) \\ & - \frac{1}{\sigma_{\theta_j}} \tilde{\theta}_j \dot{\theta}_j + \omega_j^T (\dot{\alpha}_j^c - \dot{\alpha}_j) - \frac{1}{\sigma_{\vartheta_j}} \tilde{\vartheta}_j \dot{\vartheta}_j. \end{aligned} \quad (24)$$

Similar to the derivation process of inequalities (12)–(14) in step 1, according to Lemmas 1 and 2, the following inequalities can be established:

$$z_j^T f_j \leq \theta_j \tau_j + \theta_j \frac{z_j^T z_j \varphi_j^2}{\sqrt{z_j^T z_j \varphi_j^2 + \tau_j^2}} \quad (25)$$

$$\begin{aligned} \omega_j^T (\dot{\alpha}_j^c - \dot{\alpha}_j) & \leq -\left(\frac{\eta}{\rho_j} + \frac{1}{2}\right) \omega_j^T \omega_j + \frac{\tilde{\vartheta}_j \omega_j^T \omega_j}{\sqrt{\omega_j^T \omega_j + \tau_j^2}} + \vartheta_j \tau_j \end{aligned} \quad (26)$$

$$z_j^T (z_{j+1} + \omega_j) \leq z_j^T z_j + \frac{1}{2} z_{j+1}^T z_{j+1} + \frac{1}{2} \omega_j^T \omega_j \quad (27)$$

where the nonlinear function $\varphi_j(\bar{x}_j) = 1 + \|\phi_{f_j}(\bar{x}_j)\|$.

As a consequence, substituting (8) and inequalities (25)–(27) into (24), we have the following:

$$\begin{aligned} \dot{V}_j & \leq -\sum_{m=1}^{j-1} \eta \left(\frac{1}{2} z_m^T z_m + \frac{\tilde{\theta}_m^2}{2\sigma_{\theta_m}} + \frac{\tilde{\vartheta}_m^2}{2\sigma_{\vartheta_m}} + \frac{1}{\rho_m} \omega_m^T \omega_m \right) \\ & + z_j^T \left(\frac{3}{2} z_j + \alpha_j - \dot{\alpha}_{j-1}^c + \theta_j \frac{\varphi_j^2 z_j}{\sqrt{z_j^T z_j \varphi_j^2 + \tau_j^2}} \right) \\ & - \frac{1}{\sigma_{\theta_j}} \tilde{\theta}_j \dot{\theta}_j - \frac{\eta}{\rho_j} \omega_j^T \omega_j + \vartheta_j \tau_j + \theta_j \tau_j \\ & + \frac{1}{\sigma_{\vartheta_j}} \eta \tilde{\vartheta}_j \dot{\vartheta}_j + \frac{1}{2} z_{j+1}^T z_{j+1} + \frac{b}{\varsigma} + c_{j-1}. \end{aligned} \quad (28)$$

Now, for step j , we design the VC α_j and the adaptive update law $\dot{\hat{\theta}}_j$ as

$$\alpha_j = -\frac{3}{2}z_j - \frac{\hat{\theta}_j \varphi_j^2 z_j}{\sqrt{z_j^T z_j \varphi_j^2 + \tau_j^2}} + \dot{\alpha}_{j-1}^c - \frac{1}{2}\eta z_j - \eta^2 \frac{z_j}{z_j^T z_j} \quad (29)$$

$$\dot{\hat{\theta}}_j = \sigma_{\theta_j} \frac{\varphi_j^2 z_j^T z_j}{\sqrt{z_j^T z_j \varphi_j^2 + \tau_j^2}} - \eta \hat{\theta}_j. \quad (30)$$

This means that \dot{V}_j can be further derived as

$$\begin{aligned} \dot{V}_j \leq & -\sum_{m=1}^{j-1} \eta \left(\frac{1}{2} z_m^T z_m + \frac{\tilde{\theta}_m^2}{2\sigma_{\theta_m}} + \frac{\tilde{\vartheta}_m^2}{2\sigma_{\vartheta_m}} + \frac{1}{\rho_m} \omega_m^T \omega_m \right) \\ & - \frac{1}{2} \eta z_j^T z_j - \frac{\eta}{\rho_j} \omega_j^T \omega_j + \frac{1}{\sigma_{\theta_j}} \eta \tilde{\theta}_j \hat{\theta}_j + \frac{1}{\sigma_{\vartheta_j}} \eta \tilde{\vartheta}_j \hat{\vartheta}_j \\ & - \eta^2 + \frac{1}{2} z_{j+1}^T z_{j+1} + \frac{b}{c} + c_{j-1} + \vartheta_j \tau_j + \theta_j \tau_j. \end{aligned} \quad (31)$$

Similar to inequalities (18) and (19), we have the following:

$$\frac{\eta}{\sigma_{\vartheta_j}} \tilde{\vartheta}_j \hat{\vartheta}_j \leq -\frac{\eta}{2\sigma_{\vartheta_j}} \tilde{\vartheta}_j^2 + \frac{\eta^2}{2} + \frac{\vartheta_j^4}{8\sigma_{\vartheta_j}^2} \quad (32)$$

$$\frac{\eta}{\sigma_{\theta_j}} \tilde{\theta}_j \hat{\theta}_j \leq -\frac{\eta}{2\sigma_{\theta_j}} \tilde{\theta}_j^2 + \frac{\eta^2}{2} + \frac{\theta_j^4}{8\sigma_{\theta_j}^2}. \quad (33)$$

Thus, combining (32) and (33), we can obtain the following:

$$\begin{aligned} \dot{V}_j \leq & -\sum_{m=1}^j \eta \left(\frac{1}{2} z_m^T z_m + \frac{\tilde{\theta}_m^2}{2\sigma_{\theta_m}} + \frac{\tilde{\vartheta}_m^2}{2\sigma_{\vartheta_m}} + \frac{1}{\rho_m} \omega_m^T \omega_m \right) \\ & + \frac{1}{2} z_{j+1}^T z_{j+1} + \frac{b}{c} + c_j \end{aligned} \quad (34)$$

where the positive constant c_j is defined as $c_j = \sum_{m=1}^j (\vartheta_m \tau_m + \tau_m \theta_m + (\theta_m^4/8\sigma_{\theta_m}^2) + (\vartheta_m^4/8\sigma_{\vartheta_m}^2))$.

Step n: In the last step, the dynamic \dot{z}_n can be shown as

$$\dot{z}_n = G(\bar{x}_n, t)u + f_n(\bar{x}_n) - \dot{\alpha}_{n-1}^c. \quad (35)$$

Since $G(\cdot)$ is an unknown input gain matrix, it cannot be used for subsequent controller design. For this reason, based on Assumption 2, let $a = (1/\underline{a})$ and \hat{a} be its estimate. In addition, let $\theta_n = \max\{\|W_{f_n}^*\|, \epsilon_n\}$ and $\hat{\theta}_n$ be the estimate of θ_n .

To this end, a total Lyapunov candidate is chosen as

$$V_n = V_{n-1} + \frac{1}{2} z_n^T z_n + \frac{1}{2\sigma_{\theta_n}} \tilde{\theta}_n^2 + \frac{a}{2\sigma_a} \tilde{a}^2 \quad (36)$$

where $\tilde{a} = a - \hat{a}$ and $\tilde{\theta}_n = \theta_n - \hat{\theta}_n$ denote the estimation errors, and $\sigma_{\theta_n} > 0$ and $\sigma_a > 0$ are two designed parameters. Then, by (35), we have the following:

$$\begin{aligned} \dot{V}_n = & \dot{V}_{n-1} + z_n^T (G(\cdot)u + f_n(\cdot) - \dot{\alpha}_{n-1}^c) \\ & - \frac{1}{\sigma_{\theta_n}} \tilde{\theta}_n \dot{\hat{\theta}}_n - \frac{a}{\sigma_a} \tilde{a} \dot{\hat{a}}. \end{aligned} \quad (37)$$

In view of the derivation process of inequality (12), the following inequality can be inferred:

$$z_n^T f_n \leq \theta_n \tau_n + \theta_n \frac{z_n^T z_n \varphi_n^2}{\sqrt{z_n^T z_n \varphi_n^2 + \tau_n^2}} \quad (38)$$

where $\varphi_n(\bar{x}_n)$ is defined as $\varphi_n(\bar{x}_n) = 1 + \|\phi_{f_n}(\bar{x}_n)\|$.

Based on these preparations, the control law u , the adaptive laws $\dot{\hat{\theta}}_n$ and $\dot{\hat{a}}$ will be designed separately as

$$u = -\frac{\hat{a}^2 v^T v z_n}{\sqrt{\hat{a}^2 v^T v z_n^T z_n + \tau_n^2}} \quad (39)$$

$$v = \frac{1}{2} z_n + \frac{\hat{\theta}_n \varphi_n^2 z_n}{\sqrt{z_n^T z_n \varphi_n^2 + \tau_j^2}} - \dot{\alpha}_{n-1}^c + \frac{1}{2} \eta z_n + \eta^2 \frac{z_n}{z_n^T z_n} \quad (40)$$

$$\dot{\hat{\theta}}_n = \sigma_{\theta_n} \frac{\varphi_n^2 z_n^T z_n}{\sqrt{z_n^T z_n \varphi_n^2 + \tau_n^2}} - \eta \hat{\theta}_n \quad (41)$$

$$\dot{\hat{a}} = \sigma_a z_n^T v - \eta \hat{a}. \quad (42)$$

It is noticed from Lemma 2 and (39) that

$$\begin{aligned} z_n^T G(\cdot)u & \leq -a \frac{\hat{a}^2 v^T v z_n^T z_n}{\sqrt{\hat{a}^2 v^T v z_n^T z_n + \tau_n^2}} \\ & \leq \underline{a} \tau_n - \underline{a} |\hat{a} z_n^T v| \\ & \leq \underline{a} \tau_n - z_n^T v + \underline{a} \tilde{a} z_n^T v. \end{aligned} \quad (43)$$

Further, similar to inequality (32), using Lemma 1 yields the following:

$$\frac{\eta}{\sigma_{\theta_n}} \tilde{\theta}_n \hat{\theta}_n \leq -\frac{\eta}{2\sigma_{\theta_n}} \tilde{\theta}_n^2 + \frac{\eta^2}{2} + \frac{\theta_n^4}{8\sigma_{\theta_n}^2} \quad (44)$$

$$\frac{a}{\sigma_a} \eta \tilde{a} \hat{a} \leq -\frac{a}{2\sigma_a} \eta \tilde{a}^2 + \frac{\eta^2}{2} + \frac{a^2}{8\sigma_a^2}. \quad (45)$$

Substituting inequalities (38)–(45) into (37), the time derivative \dot{V}_n in (37) will be calculated as

$$\begin{aligned} \dot{V}_n \leq & -\sum_{m=1}^n \eta \left(\frac{1}{2} z_m^T z_m + \frac{\tilde{\theta}_m^2}{2\sigma_{\theta_m}} \right) - \frac{a}{2\sigma_a} \eta \tilde{a}^2 \\ & - \sum_{m=1}^{n-1} \eta \left(\frac{\tilde{\vartheta}_m^2}{2\sigma_{\vartheta_m}} + \frac{1}{\rho_m} \omega_m^T \omega_m \right) + \frac{b}{c} + c \end{aligned} \quad (46)$$

where the positive constant is defined as

$$c = \sum_{m=1}^{n-1} \left(\vartheta_m \tau_m + \frac{\vartheta_m^4}{8\sigma_{\vartheta_m}^2} \right) + \sum_{m=1}^n \left(\tau_m \theta_m + \frac{\theta_m^4}{8\sigma_{\theta_m}^2} \right) + \frac{a^2}{8\sigma_a^2}.$$

Remark 4: Unlike the previous control schemes [16], [17], [18], [19], [20], [21], [22], [23], [24], [25], [27], [28], [29], [30], [31], [32], [33], [35], [36] using the conventional backstepping method, this study proposes a controller design framework using the DSC to simplify the calculation procedure. In detail, the traditional backstepping introduces the coordinate transformation $z_j = x_j - \alpha_{j-1}$ in the j -step iteration. This makes \dot{z}_j contain the derivative $\dot{\alpha}_{j-1}$ of the VC α_{j-1} designed in the $j-1$ -step, which will appear in the controller design in the j -step. For example, in the j th step design of [36], it is necessary to calculate the following:

$$\begin{aligned} \dot{z}_j & = \dot{x}_j - \dot{\alpha}_{j-1} \\ & = \dot{x}_j - \left(\sum_{k=1}^{j-1} \frac{\partial \alpha_{j-1}}{\partial x_k} \dot{x}_k + \sum_{k=1}^{j-1} \frac{\partial \alpha_{j-1}}{\partial x_{1d}^{k-1}} x_{1d}^{(j)} \right. \\ & \quad \left. + \frac{\partial \alpha_{j-1}}{\partial \hat{\theta}_{j-1}} \dot{\hat{\theta}}_{j-1} + \frac{\partial \alpha_{j-1}}{\partial \hat{\vartheta}_{j-1}} \dot{\hat{\vartheta}}_{j-1} \right). \end{aligned} \quad (47)$$

As can be seen from the last four terms of (47), the complex form of α_{j-1} complicates the calculation of its derivative $\dot{\alpha}_{j-1}$, especially for high-order nonlinear systems. However, by designing a NLF (7), combining (6) and (8), the DSC scheme effectively avoids calculating $\dot{\alpha}_{j-1}$ in the j -step iterative formula (21) by converting differential operations into simple algebraic operations, thereby reducing the computational burden.

Up to now, we have completed the design of the controller, and the above design process produces the following theorem.

C. Stability Analysis

Based on the NLF designed in Section III-A and the controller designed in Section III-B, this section will give the main conclusion that the system (1) is PPT stable.

Theorem 1: For the nonlinear MIMO system (1) satisfying Assumptions 1–2, under the settings of DSC with input signal (39), the VC (29), the NLF dynamics (7), and adaptive laws (8), (17), (30), (41), (42), it has the following characteristics: 1) the closed-loop system is PPT stable; and 2) the tracking error converges to the user-defined compact set $\{z_1 \mid \|z_1\| \leq \sqrt{(2b/\mu)}\}$.

Proof: Based on the definition of V_n in (36) and inequality (46), \dot{V}_n can be further simplified as

$$\dot{V}_n \leq -\eta V_n + \frac{b}{\varsigma} + c \quad (48)$$

which together with Lemma 3 implies that the equilibrium of the closed-loop system is PPT stable. Besides, according to the proof of [36], inequality (48) also means that when $t \in [0, T_e)$, the Lyapunov function V_n is bounded by

$$V_n(t) \leq e^{-dt} V_n(0) + e^{-d(t-T_e)} \frac{b}{\mu} (\varsigma(t) + 1) \quad (49)$$

and when $t > T_e$, $V_n \leq (b/\mu)$. Therefore, it follows from the definition of V_n that $(1/2)\|z_1\|^2 \leq V_1 \leq V_n$, which further indicates that the tracking error z_1 converge to the set $\{z_1 \mid \|z_1\| \leq \sqrt{(2b/\mu)}\}$ for $t > T_e$.

Moreover, in view of the boundedness and convergence of V_n , we can conclude from the definition of V_n that z_i , $\tilde{\theta}_i$, $\tilde{\vartheta}_j$, ω_j , and \tilde{a} are bounded and convergent. Based on the coordinate transformation $z_1 = x_1 - x_{1d}$ in (6), the boundedness of z_1 and x_{1d} mean that the state x_1 is bounded. This together with the definition of α_1 in (16) and Assumption 1 further indicates that α_1 is bounded. According to the equation $\omega_1 = \alpha_1^c - \alpha_1$, it can be inferred that α_1^c is also bounded. Next, by employing the coordinate transformation $z_2 = x_2 - \alpha_1^c$, we obtain that the second state x_2 is bounded, which, combined with the boundedness of $\hat{\theta}_2$, $\hat{\vartheta}_1$, and ω_1 , implies that α_2 is also bounded. It can be further obtained from equation $\omega_2 = \alpha_2^c - \alpha_2$ that α_2^c is bounded. By applying an analogous analysis procedure to the previous one, we iteratively obtain that x_j , α_j , and α_j^c are bounded. Hence, the control input u is also bounded. By applying the identical iterative analysis approach, we can also deduce that all signals within the closed-loop system converge.

This completes the stability proof. \square

Remark 5: It is worth noting that based on (16) and Lemma 3, users can freely preset the parameters b and μ without being dependent on initial values or control parameters. This feature

is an advantage over PPT controls [26], [34], where the convergence domain is determined by control parameters.

Remark 6: The DSC algorithm based on a LF was first proposed by Swaroop et al. in their work [37]. They highlighted that the stability of the system is influenced by the time constant of the filter. Hence, it is desirable to relax the requirement for filter time constants when designing control schemes using DSC frameworks. One contribution of this article is the development of a novel NLF (7), which offers two significant advantages. First, it effectively compensates for filtering errors ω_i . Second, it reduces the constraints on filter time constant ρ_i . To be more specific, if the following LF is applied:

$$\begin{cases} \rho_p \dot{\alpha}_p^c = -(\eta(t) + \frac{\rho_p}{2})\omega_p, \\ \alpha_p^c(0) = \alpha_p(0), \quad p = 1, 2, \dots, n-1. \end{cases} \quad (50)$$

Then, in the first iteration of controller design in Section III-B, the inequality (13) will be modified to

$$\omega_1^T (\dot{\alpha}_1^c - \dot{\alpha}_1) \leq -\left(\frac{\eta}{\rho_1} + \frac{1}{2}\right)\omega_1^T \omega_1 + \frac{\delta_1}{2}\omega_1^T \omega_1 + \frac{1}{2\delta_1}\vartheta_1^2 \quad (51)$$

where δ_1 is an appropriate positive constant to be selected. Simultaneously, construct the first Lyapunov function \bar{V}_1 as

$$\bar{V}_1 = \frac{1}{2}z_1^T z_1 + \frac{1}{2\sigma_{\theta_1}}\tilde{\theta}_1^2 + \frac{1}{2}\omega_1^T \omega_1. \quad (52)$$

Subsequently, according to (12), (14), (16), (17), and (19), combined with the LF (51), it can be derived that the derivative $\dot{\bar{V}}_1$ in (52) is as follows:

$$\begin{aligned} \dot{\bar{V}}_1 \leq & -\frac{1}{2}\eta z_1^T z_1 + \frac{b}{\varsigma} - \frac{1}{2\sigma_{\theta_1}}\eta\tilde{\theta}_1^2 \\ & - \left(\frac{\eta}{\rho_1} - \frac{\delta_1}{2}\right)\omega_1^T \omega_1 + \frac{1}{2}z_2^T z_2 + \bar{c}_1 \end{aligned} \quad (53)$$

where $\bar{c}_1 = (1/2\delta_1)\vartheta_1^2 + \tau_1\theta_1 + (\theta_1^4/8\sigma_{\theta_1}^2)$ is a positive constant. Next, similar derivation steps are employed for iterative design from step 2 to step n . By designing $\bar{V}_n = \sum_{m=1}^n ((1/2)z_m^T z_m + (1/2\sigma_{\theta_m})\tilde{\theta}_m^2) + \sum_{m=1}^{n-1} (1/2)\omega_m^T \omega_m + (a/2\sigma_a)\tilde{a}^2$ under LF (50), we can obtain that

$$\begin{aligned} \dot{\bar{V}}_n \leq & -\sum_{m=1}^n \eta \left(\frac{1}{2}z_m^T z_m + \frac{1}{2\sigma_{\theta_m}}\tilde{\theta}_m^2 \right) - \frac{a}{2\sigma_a}\eta\tilde{a}^2 \\ & - \sum_{m=1}^{n-1} \left(\frac{\eta}{\rho_m} - \frac{\delta_m}{2} \right) \omega_m^T \omega_m + \frac{b}{\varsigma} + \bar{c} \end{aligned} \quad (54)$$

where the positive constant \bar{c} is as follows:

$$\bar{c} = \sum_{m=1}^{n-1} \left(\frac{1}{2\delta_m}\vartheta_m^2 \right) + \sum_{m=1}^n \left(\tau_m\theta_m + \frac{\theta_m^4}{8\sigma_{\theta_m}^2} \right) + \frac{a^2}{8\sigma_a^2}.$$

To achieve the goal of PPT stability, that is, the derivative $\dot{\bar{V}}_n$ in inequality (54) further satisfies $\dot{\bar{V}}_n \leq -\eta\bar{V}_n + (b/\varsigma) + \bar{c}$, it is necessary for the coefficient $((\eta/\rho_m) - (\delta_m/2))$ associated with the filter time constant ρ_m in inequality (54) to satisfy the following:

$$\left(\frac{\eta}{\rho_m} - \frac{\delta_m}{2} \right) \geq \frac{1}{2}\eta \Rightarrow \rho_m \leq \frac{2\eta}{\delta_m + \eta} < 2 \quad (55)$$

which implies that the filter constant ρ_m will depend on the control parameter δ_m .

Furthermore, according to Lemma 3 and the stability analysis in Section III-C, the condition $\dot{\bar{V}}_n \leq -\eta\bar{V}_n + (b/\zeta) + \bar{c}$ will cause the tracking error z_1 to converge to the set $\{z_1 \mid \|z_1\| \leq \sqrt{(2b/\mu)}\}$ for $t > T_e$, where b and μ can be freely determined by the designer. However, it is worth noting that the selection of constant b must satisfy the inequality $\mu > b > \bar{c}$ (see the prerequisite for Lemma 3). Since the value of μ in (5) cannot be infinitely large, to ensure that the convergence set is as small as possible, it is usually desirable to choose a smaller value of b , which means that constant \bar{c} should be as small as possible. Therefore, based on the definition of constant \bar{c} in (54), a larger parameter δ_m should be selected to ensure that the value of the first term $(1/2\delta_m)\vartheta_m^2$ is smaller. Combining inequality (55), this further results in a smaller selection range for the time constant ρ_m of the LF (50).

However, employing the NLF (7) proposed in this article can effectively circumvent the above issue encountered with the LF (50). Specifically, the time constant ρ_m will remain unaffected by other parameters. This phenomenon is attributed to the introduction of the nonlinear term $\rho_p \hat{\vartheta}_p(\omega_p / \sqrt{\omega_p^T \omega_p + \tau_p^2})$ with adaptive law (8), which adequately compensates for the filtering error term ω_p [see inequalities (13) and (26)]. Additionally, the resulting additional constant terms $\vartheta_m \tau_m$ and $(\vartheta_m^4 / 8\sigma_{\vartheta_m}^2)$ ($m = 1, \dots, n-1$) can be minimized by selecting smaller τ_m and larger σ_{ϑ_m} , respectively, without compromising the filtering constant ρ_m . Therefore, the NLF designed in this article will allow for a greater degree of freedom in selecting filter time constant.

Corollary 1: The adaptive PPT control scheme presented in this article can also be used to address the following nonlinear MIMO system with input saturation:

$$\begin{cases} \dot{x}_p(t) = x_{p+1}(t) + f_p(\bar{x}_p(t)), & p = 1, \dots, n-1 \\ \dot{x}_n(t) = G(\bar{x}_n, t)u^s(t) + f_n(\bar{x}_n(t)) \end{cases} \quad (56)$$

where u^s represents the input signal subject to the saturation constraint, that is, $u^s = \text{sat}(u) = [\text{sat}(u_1), \dots, \text{sat}(u_m)]$ with $u = [u_1, u_2, \dots, u_m]^T$ being the actual control input to be designed. The saturation function $\text{sat}(u_i)$ has the following definition for $i = 1, 2, \dots, m$:

$$\text{sat}(u_i) = \begin{cases} u_{iM}, & u_i \geq u_{iM} \\ u_i, & u_{im} < u_i < u_{iM} \\ u_{im}, & u_i \leq u_{im} \end{cases} \quad (57)$$

where $u_{iM} > 0$ and $u_{im} < 0$ are known constants.

Next, to facilitate the subsequent controller design, similar to [41], we will introduce a smooth function $H(u_i)$ to approximate the saturation function $\text{sat}(u_i)$, which is defined as

$$H(u_i) = \begin{cases} u_{iM} \tanh\left(\frac{u_i}{u_{iM}}\right), & u_i \geq 0 \\ u_{im} \tanh\left(\frac{u_i}{u_{im}}\right), & u_i < 0. \end{cases} \quad (58)$$

Then, by using the Lagrange mean value theorem yields the following:

$$\text{sat}(u_i) = H(u_i) + \zeta(u_i) = H'_{u_i} u_i + \zeta(u_i) \quad (59)$$

where $\zeta(u_i) = \text{sat}(u_i) - H(u_i)$ satisfies $|\zeta(u_i)| \leq \max\{u_{iM}(1 - \tanh(1)), u_{im}(\tanh(1) - 1)\} \triangleq \zeta_{iM}$, $H'_{u_i} = (\partial H(u_i) / \partial u_i)|_{u_i=u'_i}$ and $u'_i = \pi_i u_i + (1 - \pi_i)u_{i0}$ with $u_{i0} = 0$, $0 < \pi_i < 1$ and $0 < \underline{H}_m \leq H'_{u_i} \leq 1$.

Therefore, the dynamic system (56) can be rewritten as

$$\begin{cases} \dot{x}_p(t) = x_{p+1}(t) + f_p(\bar{x}_p(t)), & p = 1, \dots, n-1 \\ \dot{x}_n(t) = G(\bar{x}_n, t)H'_u u + G(\bar{x}_n, t)\bar{\zeta}(u) + f_n(\bar{x}_n) \end{cases} \quad (60)$$

where $H'_u = \text{diag}\{H'_{u_1}, H'_{u_2}, \dots, H'_{u_m}\}$ and $\bar{\zeta}(u) = [\zeta(u_1), \zeta(u_2), \dots, \zeta(u_m)]^T$. Note that although input saturation makes the expression of the last S-D \dot{x}_n of system (60) different from the studied system (1), both have the same properties. This is mainly reflected in two aspects. First, since both G and H'_u are bounded, there are two unknown positive constants \underline{a}_1 and \bar{a}_1 such that

$$\underline{a}_1 \leq \|G(\bar{x}_n, t)H'_u\| \leq \bar{a}_1 \quad (61)$$

holds. In addition, let $\bar{f}(\bar{x}_n(t)) = G(\bar{x}_n, t)\bar{\zeta}(u) + f_n(\bar{x}_n(t))$ and use the NNs similar to (4) to obtain its approximate form

$$\bar{f}(\bar{x}_n(t)) = W_{\bar{f}_n}^{*T} \bar{\phi}_{\bar{f}_n}(\bar{x}_n) + \varepsilon_{\bar{f}_n}(\bar{x}_n). \quad (62)$$

By leveraging the aforementioned characteristics, it can also obtain the PPT stability performance under saturation constraints through an iterative design process, similar to Section III-B, for the transformation system (60). For the sake of brevity, it will not be repeated.

IV. EXAMPLE AND SIMULATION

To verify the validity of the presented algorithm, this section will consider the following a two-degree-of-freedom robot manipulator with unknown model dynamics:

$$\begin{cases} \dot{x}_1 = x_2 \\ D(x_1)\dot{x}_2 + C(x_1, x_2)x_2 + G(x_1) + F(x_1, x_2) = u \end{cases} \quad (63)$$

where $x_1 = [x_{11}, x_{12}]^T$ denotes the joint position, $x_2 = [x_{21}, x_{22}]^T$ is the velocity vectors, and u denotes the system input. $D(\cdot) = [D_{ij}]_{2 \times 2}$ is the inertia matrix, where $D_{11} = m_1 l_{c1}^2 + m_2(l_1^2 + l_{c2}^2 + 2l_1 l_{c2} \cos(x_{12})) + I_1 + I_2$, $D_{12} = D_{21} = m_2(l_{c2}^2 + l_1 l_{c2} \cos(x_{12})) + I_2$, and $D_{22} = m_2 l_{c2}^2 + I_2$. $C(\cdot) = [C_{ij}]_{2 \times 2}$ is the centripetal-Coriolis matrix with $C_{11} = -m_2 l_1 l_{c2} x_{22} \sin(x_{12})$, $C_{12} = -m_2 l_1 l_{c2} \sin(x_{12})(x_{21} + x_{22})$, $C_{21} = m_2 l_1 l_{c2} x_{21} \sin(x_{12})$ and $C_{22} = 0$. The gravity vector $G(x_1) = [G_1, G_2]^T$ is defined by $G_1 = (m_1 l_{c1} + m_2 l_1)g \cos(x_{11}) + m_2 l_{c2} g \cos(x_{11} + x_{12})$ and $G_2 = m_2 l_{c2} g \cos(x_{11} + x_{12})$. $F = [0.5 \sin(x_{11}), 0.5 \sin(x_{12})]^T$ denotes a nonlinear function. The parameter values in the above matrices are given as $m_1 = m_2 = 1 \text{ kg}$, $l_1 = l_2 = 1 \text{ m}$, $l_{c1} = l_{c2} = 0.5 \text{ m}$, $I_1 = I_2 = 0.5 \text{ kg} \cdot \text{m}$, $g = 9.81 \text{ m/s}^2$.

Let the desired trajectory be $x_{1d} = [x_{1d1}, x_{1d2}]^T \text{ rad}$ with $x_{1d1} = -2 + 3 \sin(2t + \pi/2)$ and $x_{1d2} = 2 \sin(2t + \pi/2) - 1.2$. Note that the robot manipulator corresponds to the dynamic model (1) considered in this article when $n = 2$. Therefore, on the basis of the proposed PPT control scheme, we can design the NLF, the adaptive laws, and the controller for the robot manipulator correspond to those provided in Section III.

TABLE II
TRANSIENT VALUES OF TRACKING ERROR UNDER NLF

Case 1: Controller parameters $\chi = [1, 5, 0.3]$	Initial Value	$\ z_1\ _{t=T_e}$
	$x(0) = [3, -2, 1, -1]$	$z_{11} = -0.0696,$ $z_{12} = -0.0461,$ $\ z_1\ \approx 0.0835$
Case 2: Initial Value $x(0) = [3, -2, 1, -1]$	Controller parameters	$\ z_1\ _{t=T_e}$
	$\sigma_{\vartheta_1} = 1$ $\sigma_{\theta} = 5$ $\sigma_a = 0.3$	$z_{11} = -0.0696,$ $z_{12} = -0.0461,$ $\ z_1\ \approx 0.0835$
	$\sigma_{\vartheta_1} = 5$ $\sigma_{\theta} = 2$ $\sigma_a = 0.5$	$z_{11} = -0.0706,$ $z_{12} = -0.0530,$ $\ z_1\ \approx 0.0835$

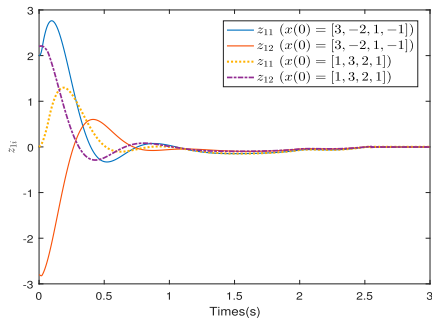


Fig. 2. Trajectories of errors z_{1i} under different initial values.

Next, to validate the efficacy and superiority of the algorithm presented in Theorem 1, we will conduct simulation comparisons from two aspects as follows.

- 1) One aspect of comparison is to confirm that the presented NLF-based scheme guarantees convergence of the tracking error to the user-defined compact set at the preset time, irrespective of the initial values, and control parameters of system.
- 2) Additionally, we will show the superiority of the proposed NLF-based scheme has better stability than using the LF.

A. Part I

Verify that the convergence of the tracking error independent of the initial values and control parameters.

First, for simulation implementation, let $T_e = 2$ s, $\mu = 0.25$, $b = 0.001$, $d = 10$, and $\rho_1 = 2$. Then, according to Theorem 1, the tracking error $z_1 = x_1 - x_{1d} \triangleq [z_{11}, z_{12}]$ will converge the predefined set $\{z_1 | \|z_1\| \leq \sqrt{2b/\mu} = 0.0894\}$ in the prescribed settling time $T_e = 2$. In addition, the unknown dynamics $-D^{-1}(Cx_2 + G + F)$ is approximated by choosing the neuron number of the RBF NNs being 11, the bandwidth being $v = 3$ and the centers being evenly spaced in the interval $[-2.5, 2.5]$. Let $x = [x_1, x_2]^T$ and $\chi = [\sigma_{\vartheta_1}, \sigma_{\theta}, \sigma_a]$. Next, two cases of simulation comparisons are given as follows.

Case 1: Choose the controller parameters as $\chi = [1, 5, 0.3]$. Perform simulation comparisons with different initial values $x(0) = [3, -2, 1, -1]^T$ and $x(0) = [1, 3, 2, 1]^T$.

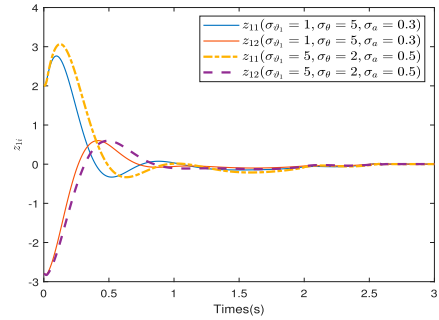


Fig. 3. Trajectories of errors z_{1i} under different controller parameters.

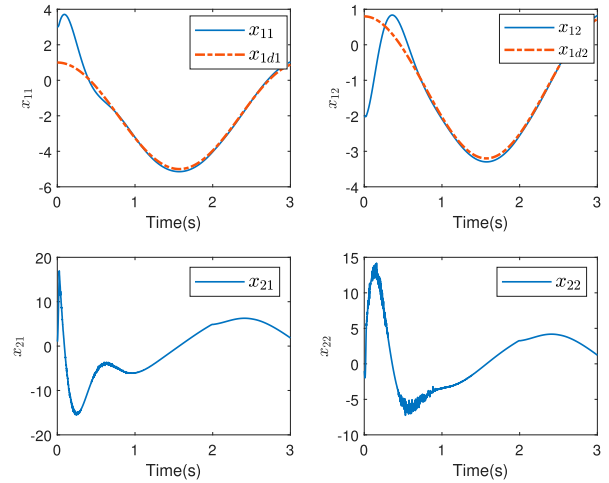


Fig. 4. Trajectories of state variables x_{ij} and tracking signals.

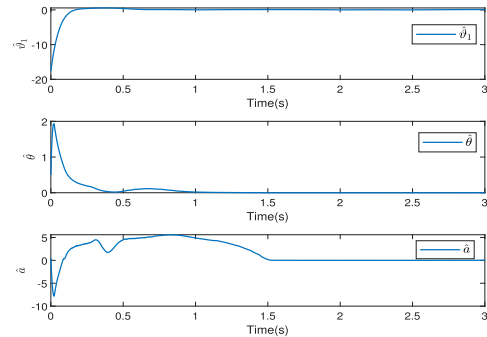
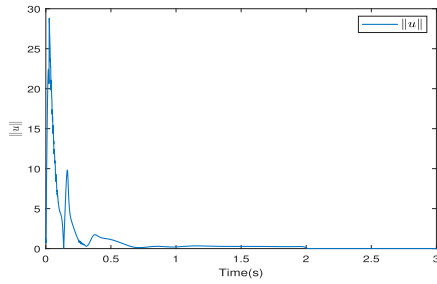
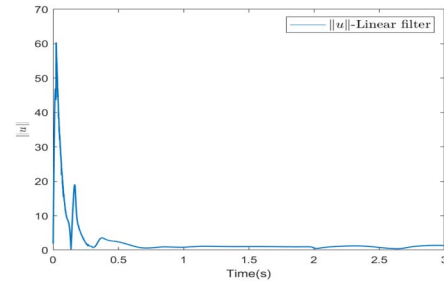
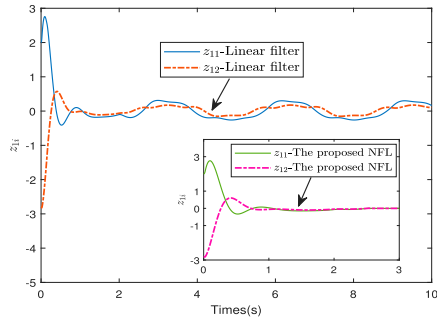


Fig. 5. Trajectories of adaptive laws.

Case 2: Select the initial value $x(0) = [3, -2, 1, -1]$ and conduct simulation comparisons under different control parameters $\chi = [1, 5, 0.3]$ and $\chi = [5, 2, 0.5]$.

Using these given parameters, Figs. 2–6 illustrate the simulation results. Fig. 2 displays tracking error trajectories with various initial conditions, while Fig. 3 compares tracking error trajectories with different controller parameters. Additionally, the transient values of tracking errors in Figs. 2 and 3 are given in Table II. Figs. 4–6 depict the trajectories of system states and adaptive laws under $x(0) = [3, -2, 1, -1]$ and $\chi = [1, 5, 0.3]$. From Table II, at the settling time $t = 2$, there is always $\|z_1\| < 0.0894$, regardless of initial values and controller parameters.

Fig. 6. Trajectory of the input signal norm $\|u\|$.Fig. 8. Trajectories of the input norm $\|u_i\|$ using the LF.Fig. 7. Compare of errors z_{1i} using the LF and the proposed NLF.

This, along with Figs. 2 and 3, shows that using the presented PPT control scheme, the tracking error can converge to the user-defined compact set at the preset settling time independent of system initial values and controller parameters. This feature is superior to the existing PPT control algorithms [31], [34] that are limited to Euler–Lagrange dynamics or SISO systems. Additionally, the convergence set of tracking errors in [31] and [34] is also determined by the controller parameters. Further, as can be seen from Figs. 4 and 5, the system state and adaptive laws are all bounded. As indicated in Fig. 6, the input signal is also a bounded variable. As a consequence, the validity of the proposed PPT stability scheme with a novel NLF for uncertain nonlinear MIMO system is verified by Figs. 2–5.

B. Part II

A comparison between the proposed NLF-based scheme and one employing LF.

By using the initial value $x(0) = [3, -2, 1, -1]^T$, controller parameter $\chi = [1, 5, 0.3]$, and keeping other parameters unchanged, if the LF is used for controller design, the trajectories of the tracking error and input signal are illustrated in Figs. 7 and 8, respectively (due to limited space, only the trajectories of key variables are provided here). It can be seen that the tracking errors in Fig. 7, unlike the one in Fig. 2 after $t = 2$ s, do not exhibit convergence to a small neighborhood of the origin, but instead oscillating around the origin. This is further shown that under the same filter time constant and control parameters, the stability performance and convergence accuracy obtained by the developed NLF-based PPT control scheme are superior than that of the LF [34].

V. CONCLUSION

In this study, we thoroughly investigated the adaptive PPT stability of nonlinear high-order MIMO systems with unknown nonlinear functions and unknown input gain matrices. To address the inherent computational complexity, a novel DSC framework had been introduced. Additionally, we have designed a new NLF, equipped with an adaptive parameter estimator, which effectively compensates for filtering errors while also providing more flexibility in setting the filter time constant. By leveraging both neural approximator and adaptive technology, our proposed algorithm appropriately compensated for system uncertainties. The key achievement of this research ensured PPT stability for the closed-loop system and enabled the tracking error to converge to a user-defined residual set within the settling time. Notably, this performance was achieved independently of the system’s initial values and control parameters.

Note that the control input matrix in system (1) is required to be positive definite. However, for many practical physical systems, their control matrices may be constantly changing or not square matrices. Therefore, developing a PT control schemes that allow the direction of the control input matrix to be unknown is a direction worthy of future research.

REFERENCES

- [1] L. Fraguela, M. T. Angulo, J. A. Moreno and L. Fridman, “Design of a prescribed convergence time uniform robust exact observer in the presence of measurement noise,” in *Proc. IEEE 1st IEEE Conf. Decis. Control (CDC)*, 2012, pp. 6615–6620.
- [2] Y. Song, Y. Wang, J. Holloway, and M. Krstic, “Time-varying feedback for regulation of normal-form nonlinear systems in prescribed finite time,” *Automatica*, vol. 83, pp. 243–251, 2017.
- [3] H. Ye and Y. Song, “Prescribed-time control for linear systems in canonical form via nonlinear feedback,” *IEEE Trans. Syst., Man, Cybern.: Syst.*, vol. 53, no. 2, pp. 1126–1135, Feb. 2023.
- [4] R. Liu, H. Wang, and W. Li, “Prescribed-time stabilization and inverse optimal control of stochastic high-order nonlinear systems,” *Sci. China Inf. Sci.*, vol. 67, 2024, Art. no. 122202.
- [5] D. Steeves, L. Camacho-Solorio, M. Benosman, and M. Krstic, “Prescribed-time tracking for triangular systems of reaction-diffusion PDEs,” *IFAC-PapersOnLine*, vol. 53, no. 2, pp. 7629–7634, 2020.
- [6] Y. Li, X. Zheng, and K. Li, “Prescribed-time adaptive intelligent formation controller for nonlinear multi-agent systems based on time-domain mapping,” *IEEE Trans. Artif. Intell.*, vol. 5, no. 4, pp. 1778–1790, Apr. 2024.
- [7] K. Zhang, B. Zhou, X. Yang, and G. Duan, “Prescribed-time leader-following consensus of linear multi-agent systems by bounded linear time-varying protocols,” *Sci. China Inf. Sci.*, vol. 67, 2024, Art. no. 112201.
- [8] L. Liu, C. Zhu, Y. -J. Liu, and S. Tong, “Adaptive finite-time neural constrained control for nonlinear active suspension systems based on

- the command filter," *IEEE Trans. Artif. Intell.*, vol. 3, no. 2, pp. 218–227, Apr. 2022.
- [9] P. Wang, C. P. Yu, and Y. J. Pan, "Finite-time output feedback cooperative formation control for marine surface vessels with unknown actuator faults," *IEEE Trans. Control Netw. Syst.*, vol. 10, no. 2, pp. 887–899, Jun. 2023.
- [10] J. P. Yu, C. Fu, J. P. Liu, and Y. M. Ma, "Barrier Lyapunov function-based finite-time dynamic surface control for output-constrained nonstrict-feedback systems," *J. Syst. Sci. Complexity*, vol. 36, pp. 524–539, Apr. 2023.
- [11] S. Sun, C. L. Philip Chen, and S. C. Tong, "A novel full errors fixed-time control for constraint nonlinear systems," *IEEE Trans. Autom. Control*, vol. 68, no. 4, pp. 2568–2575, Apr. 2023.
- [12] G. Cui, H. Xu, J. Yu, Q. Ma, and M. Jian, "Event-triggered fixed-time adaptive fuzzy control for non-triangular nonlinear systems with unknown control directions," *IEEE Trans. Artif. Intell.*, vol. 5, no. 5, pp. 2397–2409, May 2024.
- [13] M. L. C. Ki Ahn, B. Zhang, and A. Fu, "Fixed-time anti-saturation cooperative control for networked fixed-wing unmanned aerial vehicles considering actuator failures," *IEEE Trans. Aerosp. Electron. Syst.*, vol. 59, no. 6, pp. 8812–8825, Dec. 2023.
- [14] P. Wang, C. P. Yu, M. L. Lv, and J. D. Cao, "Adaptive fixed-time optimized formation control using reinforcement learning for nonlinear multiagent systems," *IEEE Trans. Netw. Sci. Eng.*, vol. 11, no. 2, pp. 1729–1743, Mar./Apr. 2024.
- [15] F. Wang, Z. Ma, C. Zhou, z. Zhang, C. Hua, and Q. Zou, "Fixed-time controller design for a quadrotor UAV with asymmetric output error constraints," *J. Syst. Sci. Complexity*, vol. 36, pp. 1981–2000, Oct. 2023.
- [16] H. Ye and Y. Song, "Prescribed-time tracking control of MIMO nonlinear systems under non-vanishing uncertainties," *IEEE Trans. Autom. Control*, vol. 68, no. 6, pp. 3664–3671, Jun. 2023.
- [17] N. Espitia and W. Perruquetti, "Predictor-feedback prescribed-time stabilization of LTI systems with input delay," *IEEE Trans. Autom. Control*, vol. 67, no. 6, pp. 2784–2799, Jun. 2022.
- [18] P. Krishnamurthy, F. Khorrami, and M. Krstic, "Prescribed-time stabilization of nonlinear strict-feedback-like systems," in *Proc. Amer. Control Conf. (ACC)*, 2019, pp. 3081–3086.
- [19] P. Krishnamurthy, F. Khorrami, and M. Krstic, "A dynamic high-gain design for prescribed-time regulation of nonlinear systems," *Automatica*, vol. 115, 2020, Art. no.108860.
- [20] D. Tran and T. Yucelen, "Finite-time control of perturbed dynamical systems based on a generalized time transformation approach," *Syst. & Control Lett.*, vol. 136, 2020, Art. no. 104605.
- [21] B. Zhou and Y. Shi, "Prescribed-time stabilization of a class of nonlinear systems by linear time-varying feedback," *IEEE Trans. Autom. Control*, vol. 66, no. 12, pp. 6123–6130, Dec. 2021.
- [22] W. Li and M. Krstic, "Stochastic nonlinear prescribed-time stabilization and inverse optimality," *IEEE Trans. Autom. Control*, vol. 67, no. 3, pp. 1179–1193, Mar. 2022.
- [23] Y. D. Song, H. F. Ye, and Frank L. Lewis, "Prescribed-time control and its latest developments," *IEEE Trans. Syst., Man, Cybern.: Syst.*, vol. 53, no. 7, pp. 4102–4116, Jul. 2023.
- [24] P. Krishnamurthy, F. Khorrami, and M. Krstic, "Robust adaptive prescribed-time stabilization via output feedback for uncertain nonlinear strict feedback-like systems," *Eur. J. Control*, vol. 55, pp. 14–23, 2020.
- [25] C. Hua, P. Ning, and K. Li, "Adaptive prescribed-time control for a class of uncertain nonlinear systems," *IEEE Trans. Autom. Control*, vol. 67, no.11, pp. 6159–6166, Nov. 2022.
- [26] G. W. Zuo and Y. J. Wang, "Adaptive prescribed finite time control for strict-feedback systems," *IEEE Trans. Autom. Control*, vol. 68, no. 9, pp. 5729–5736, Sep. 2023.
- [27] Z. W. Wang, B. Liang, Y. C. Sun, and T. Zhang, "Adaptive fault-tolerant prescribed-time control for teleoperation systems with position error constraints," *IEEE Trans. Ind. Inform.*, vol. 16, no. 7, pp. 4889–4899, Jul. 2020.
- [28] K. Zhao, Y. Song, and Y. Wang, "Regular error feedback based adaptive practical prescribed time tracking control of normal-form nonaffine systems," *J. Franklin Inst.*, vol. 356, pp. 2759–2779, Feb. 2019.
- [29] K. Zhao, Y. Song, and L. Chen, "Tracking control of nonlinear systems with improved performance via transformational approach," *Int. J. Robust Nonlinear Control*, vol.29, no. 6, pp. 1789–1806, Apr. 2019.
- [30] P. Krishnamurthy and F. Khorrami, "Practical prescribed-time stabilization and tracking for uncertain nonlinear systems with disturbance inputs," in *Proc. 60th IEEE Conf. Decis. Control (CDC)*, Austin, TX, USA, 2021, pp. 4588–4593.
- [31] J. Wang, Q. Gong, K. Huang, Z. Liu, C. L. P. Chen, and J. Liu, "Event-triggered prescribed settling time consensus compensation control for a class of uncertain nonlinear systems with actuator failures," *IEEE Trans. Neural Netw. Learn. Syst.*, vol. 34, no. 9, pp. 5590–5600, Sep. 2023.
- [32] K. Zhang, B. Zhou, M. Hou, and G. R. Duan, "Practical prescribed-time stabilization of a class of nonlinear systems by event-triggered and self-triggered control," *IEEE Trans. Autom. Control*, vol. 69, no. 5, pp. 3426–3433, May 2024.
- [33] K. Zhao, Y. Song, T. Ma, and L. He, "Prescribed performance control of uncertain Euler–Lagrange systems subject to full-state constraints," *IEEE Trans. Neural Netw. Learn. Syst.*, vol.29, no. 8, pp. 3478–3489, Aug. 2018.
- [34] Y. Cao, J. F. Cao, and Y. D. Song, "Practical prescribed time control of Euler-Lagrange systems with partial/full state constraints: A settling time regulator-based approach," *IEEE Trans. Cybern.*, vol. 52, no. 12, pp. 13096–13105, Dec. 2022.
- [35] Z. W. Wang, Hak. K. Lam, Z. Chen, B. Liang, and T. Zhang, "Adaptive prescribed-time control for uncertain nonlinear systems with non-affine actuator failures," *Int. Federation Autom. Control (IFAC)*, vol. 53, no. 2, pp. 3821–3828, 2020.
- [36] Z. Wang et al., "Adaptive event-triggered control for nonlinear systems with asymmetric state constraints: A prescribed-time approach," *IEEE Trans. Autom. Control*, vol. 68, no. 6, pp. 3625–3632, Jun. 2023.
- [37] D. Swaroop, J. K. Hedrick, P. P. Yip, and J. C. Gerdes, "Dynamic surface control for a class of nonlinear systems," *IEEE Trans. Autom. Control*, vol. 45, no. 10, pp. 1893–1899, Oct. 2000.
- [38] C. Liu, B. Niu, L. Liu, X. Zhao, H. Wang, and H. Duan, "Event-triggered adaptive bipartite asymptotic tracking control using intelligent technique for stochastic nonlinear multi-agent systems," *IEEE Trans. Artif. Intell.*, vol. 4, no. 6, pp. 1616–1626, Dec. 2023.
- [39] P. Wang, C. P. Yu, and J. Sun, "Decentralized adaptive tracking control for nonlinear large-scale systems with unknown control directions," *Int. J. Robust Nonlinear Control*, vol. 32, no. 2, pp. 620–648, Feb. 2022.
- [40] Q. Liu, D. Li, S. S. Ge, and Z. Ouyang, "Adaptive feedforward neural network control with an optimized hidden node distribution," *IEEE Trans. Artif. Intell.*, vol. 2, no. 1, pp. 71–82, Feb. 2021.
- [41] H. F. Min, S. Y. Xu, and Z. Q. Zhang, "Adaptive finite-time stabilization of stochastic nonlinear systems subject to full-state constraints and input saturation," *IEEE Trans. Autom. Control*, vol. 66, no. 3, pp. 1306–1313, Mar. 2021.